

# Factors influencing the temporal characteristics of coherent wake field harmonic emission from solid surfaces

Rainer Hörlein<sup>a,b</sup>, Yutaka Nomura<sup>a,c</sup>, Sergey G. Rykovanov<sup>a,d</sup>, Ferenc Krausz<sup>a,b</sup>,  
George D. Tsakiris<sup>a</sup>

<sup>a</sup>Max-Planck-Institut für Quantenoptik,  
Hans-Kopfermann-Str. 1, 85748 Garching, Germany;

<sup>b</sup>Sektion Physik der Ludwig-Maximilians-Universität München,  
Am Coulombwall 1, 85748 Garching, Germany;

<sup>c</sup>Institute for Solid State Physics, University of Tokyo,  
Kashiwanoha 5-1-5, Kashiwa, Chiba 277-8581, Japan;

<sup>d</sup>Moscow Physics Engineering Institute,  
Kashirskoe shosse 31, 115409 Moscow, Russia

## ABSTRACT

The temporal characteristics of the harmonic emission from solid targets irradiated with intense laser pulses is examined in detail. In the case where the Coherent Wake Emission mechanism is dominant it is found that indeed the harmonics thus produced possess a frequency chirp resulting in non Fourier-Transform-Limited pulses. A simple model explains the underlying physics while Particle-In-Cell simulations support the conclusions drawn.

**Keywords:** Harmonic emission, Laser-plasma interaction, Attosecond pulse generation

## 1. INTRODUCTION

The generation of coherent high harmonic radiation from the interaction of relativistically intense femtosecond laser pulses with solid targets promises the generation of attosecond pulses orders of magnitude more brilliant than those generated from gaseous media.<sup>1-3</sup> Such pulses would, for the first time, enable researchers to explore a whole new class of attosecond time resolution XUV-pump XUV-probe type experiments not accessible with the relatively weak gas-harmonic sources available today.<sup>4</sup> It was recently demonstrated experimentally that the harmonics generated from the interaction of a relativistically intense laser pulse with a solid target are coherent giving rise to a train of attosecond pulses.<sup>5</sup> The temporal structure of the harmonics emitted from the target was characterized using the volume autocorrelation technique following a scheme previously employed for the characterization of gas-harmonics.<sup>6</sup> The measured duration of the individual attosecond pulses was found to be longer than what was expected from a coherent superposition of the harmonic emission suggesting that there is an intrinsic mechanism contributing to the temporal broadening of the individual attosecond pulses. In this paper we examine in more detail the nature of the Coherent Wake Emission (CWE) mechanism, which was responsible for the harmonic emission observed in<sup>5</sup> and we find that indeed the harmonics thus produced possess a frequency chirp resulting in non Fourier-Transform-Limited (FTL) pulses.

## 2. COHERENT WAKE EMISSION

In contrast to the Relativistic Oscillating Mirror (ROM) harmonics which are generated at the surface of the target and have been studied theoretically as well as experimentally in numerous publications,<sup>1,2,7-13</sup> coherent wake emission (CWE) is a bulk process, i.e. the harmonics are generated inside the overdense bulk plasma. While the fact that harmonics can be generated inside an overdense plasma gradient is known since the late 1970s<sup>14-16</sup> it was only recently that the generation process for femtosecond pulses was adequately clarified.<sup>3,17</sup> Today, the

---

Send correspondence to Rainer Hörlein  
E-mail: rainer.hoerlein@mpq.mpg.de

generation of harmonics inside the bulk plasma is attributed to bunches of hot electrons (Brunel electrons<sup>18</sup>), which are first pulled out of the plasma by the component of the laser electric field perpendicular to the target surface to be hurled back inside when the field reverses. The hot electrons propagate through the density gradient and excite plasma waves in their wake. These plasma waves can, under certain conditions, undergo linear mode conversion and radiate electromagnetic waves. This process is essentially inverse resonance absorption and has been discussed in detail by Sheng et al.<sup>19</sup> It is important to note that CWE harmonics can only be generated in plasmas that have a finite scale-length. If the density profile is step-like it cannot generate any harmonics<sup>20</sup> because plasma waves with frequencies corresponding to the harmonics cannot be excited. Under very high contrast interactions this can lead to the suppression of the emission of lower order CWE harmonics.<sup>21</sup>

The indirect generation of harmonics via hot electrons and plasma waves results in several unique properties of the generated harmonics which distinguish them clearly from the ROM harmonics. Most importantly the CWE harmonics can be generated at sub-relativistic intensities ( $a_0 \ll 1$ ) as low as  $1 \times 10^{16} \text{Wcm}^{-2}$ .<sup>3</sup> Besides the intensity necessary for the generation there are two more interesting differences between CWE and ROM mechanisms. The highest generated harmonic for CWE does not depend on the laser intensity but rather on the properties of the target material and the mechanism itself introduces two kinds of chirp on the emitted harmonics. Both effects, the cutoff and the chirp, can be understood when looking at the harmonic generation mechanism in a little more detail.

Let us consider the cutoff first. As has been mentioned above the harmonics are generated via mode conversion of plasma waves excited by hot electrons in the pre-plasma gradient of the target. The wavelength of the generated harmonic is thus directly related to the frequency of the excited plasma wave which, in turn, is a function of the local electron density. This means that each harmonic is generated at a different depth within the density gradient and that the highest generated harmonic  $q_{co}$  can be calculated from the maximum electron density of the target and the laser wavelength (with its corresponding critical density  $n_c$ ). It is:

$$q_{co} \approx \sqrt{\frac{n_{\max}}{n_c}}. \quad (1)$$

For the target materials typically used in experiments  $q_{co}$  lies between 14 for low-density plastics like polymethylmetacrylate (PMMA) and 20 for BK7-glass or fused silica. In principle higher cutoff harmonics should be achievable from high-density lead glass or metal targets. The dependence of the spectral cutoff on the target density for CWE harmonics has been demonstrated in several publications.<sup>5, 10, 22</sup>

The fact that the harmonics are generated indirectly via Brunel electrons exciting plasma waves inside the target leads to two different kinds of chirp, a harmonic chirp inside each harmonic and an atto-chirp between the harmonics. The harmonic chirp originates from the fact that the Brunel electrons spend different amounts of time in the vacuum before they are injected into the plasma gradient depending on the instantaneous laser intensity. This leads to the emission of unequally spaced attosecond pulses as has been shown in detailed PIC simulations by F. Quéré et al.<sup>20</sup> Experimentally this unequal spacing is observed as a broadening of the individual harmonics that can be at least partially compensated by properly chirping the incident laser pulse to minimize the unequal spacing.<sup>3, 20, 23</sup>

In contrast to the harmonic-chirp the origin of the atto-chirp, i.e. the chirp between the individual harmonics, lies in the fact that the wavelength of the generated harmonic relies on the local electron density. Higher harmonics are generated further inside the density gradient and thus have to travel a longer distance to the target surface than the lower orders. This effect is demonstrated both in the results of a PIC simulation (a) as well as schematically (b) in figure 1. The simulation shows the currents inside a plasma gradient of length  $L = 0.2\lambda_L$  as a function of position and frequency. Higher frequency currents are resonant deeper inside the target where the density is higher. At the same time the simulation also nicely shows the cutoff for the generation of plasma harmonics. The highest resonant frequency is  $14 \omega_L$  which corresponds to the peak density of  $n_{\max} = 200n_c$  used in the simulation (see equation 1).

The attosecond-pulses generated by the superposition of the individual CWE harmonics will carry a chirp depending on the scale-length of the preplasma density gradient and the velocity of the Brunel electrons causing the excitation of the plasma oscillations. To quantify this chirp and help in interpreting the results of the direct

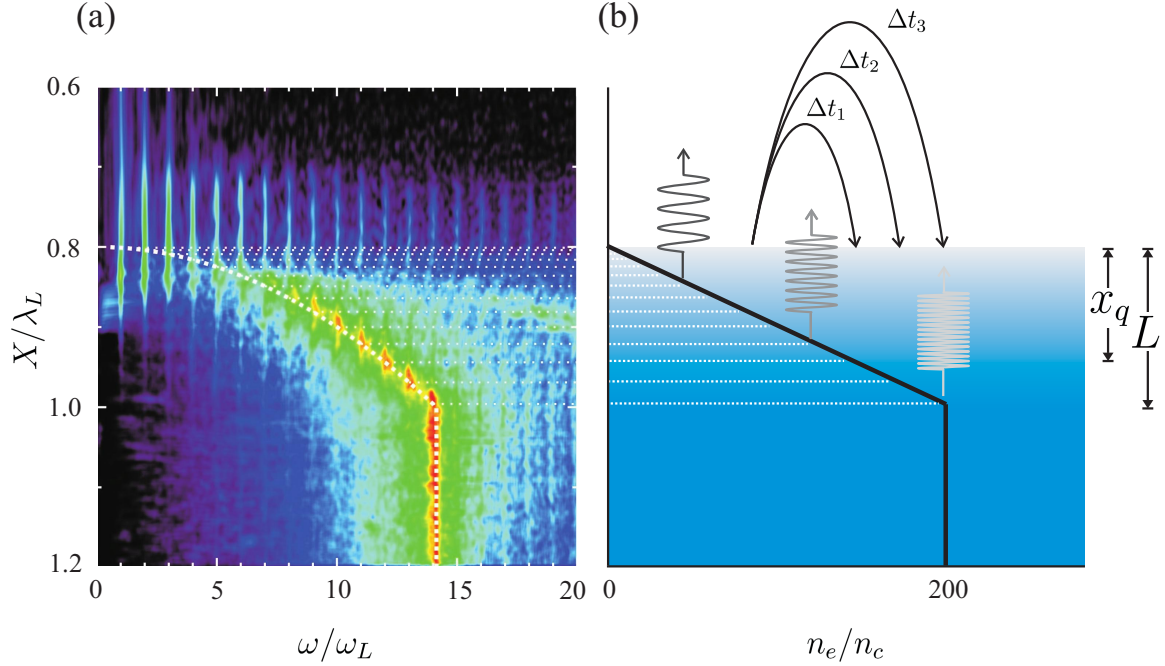


Figure 1. Figure illustrating the basic features of CWE harmonics. Panel (a) shows the nonlinear currents inside a target with a maximum density  $n_{\max} = 200n_c$  and a linear density ramp of length  $L = 0.2\lambda_L$  irradiated with a peak laser intensity of  $a_0 = 1.5$  as obtained from a PIC simulation. Different frequency currents are seen to be resonant at different depth inside the density ramp corresponding to those positions where the local plasma frequency  $\omega_p = q\omega_L$ . The harmonic cutoff predicted by equation 1 is also visible. In (b) the two origins of chirp in CWE harmonics are shown schematically. While the fact that harmonics are generated at different depth inside the target leads to a chirping of the individual attosecond pulses the different excursion times of the electrons as a function of the driving laser intensity leads to unequal spacing of the individual as-pulses.

XUV-autocorrelation of the generated attosecond pulses<sup>5</sup> we have developed a simple model for the atto-chirp which shall be discussed in the following paragraphs.

The starting point for the model is a linear density gradient of length  $L$  over which the electron density in the target rises from zero to  $n_{\max}$  (see figure 1). The density as a function of position  $x$  can then be written as

$$n_e(x) = \frac{x}{L}n_{\max}. \quad (2)$$

Considering that the relation between the local electron density and plasma frequency is  $\omega_p \propto n_e^2$  it is possible to calculate the position  $x(q)$  inside the gradient at which the individual harmonics are generated:

$$x(q) = L \frac{n_c}{n_{\max}} q^2 \quad (3)$$

Note that this parabolic behavior with harmonic number is also nicely reproduced by the PIC simulation shown in figure 1. To calculate the relative phase between the individual harmonics from the position at which they are generated two things have to be taken into account: the time it takes for the Brunel electrons to travel to the point in the gradient where the harmonic of interest is generated and the additional phase shift originating from the time it takes for each harmonic to propagate out of the gradient. In general terms the phase accumulated by the  $q$ -th harmonic is

$$\phi(q) = 2\pi \frac{L}{\lambda_L} \frac{n_c}{n_{\max}} q^3 \left[ \frac{c}{v_e \cos(\Theta_{\text{in},e})} + \frac{c}{v_{\text{ph}} \cos(\Theta_{\text{out,ph}})} \right], \quad (4)$$

where the first term in the brackets accounts for the electron propagation into ( $v_e$  is the electron velocity and  $\Theta_{\text{in},e}$  the angle of incidence (AOI) of the electrons onto the target) and the second for the propagation of the

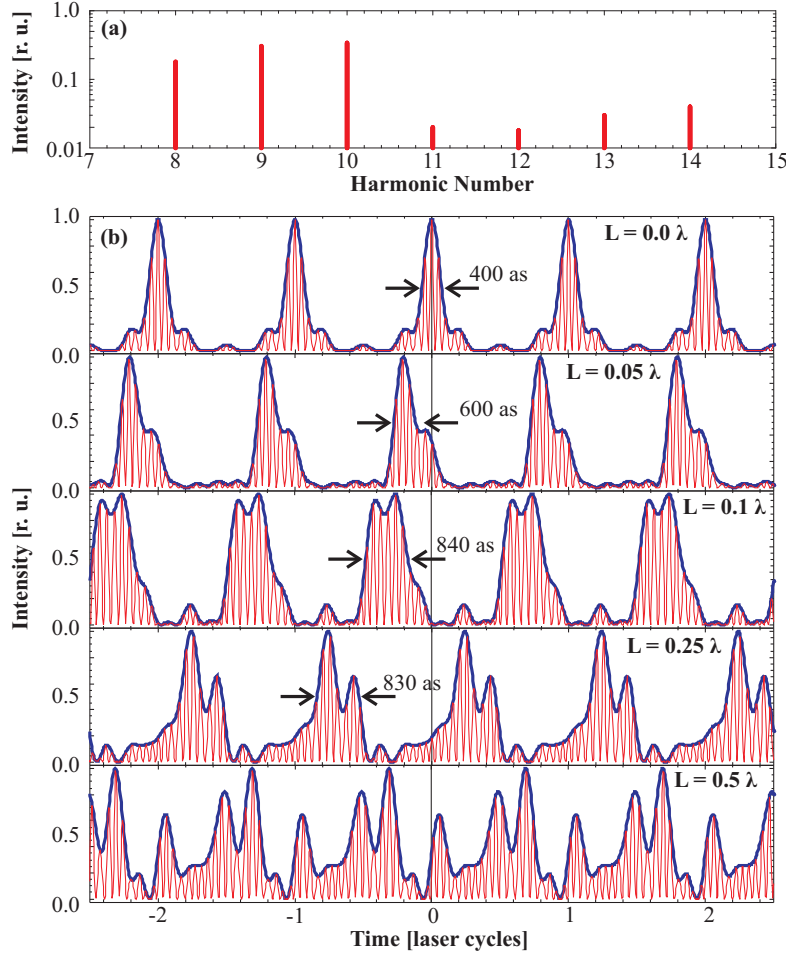


Figure 2. Calculation of chirped attosecond pulse trains. (a) Shows the power-spectrum used in the calculations. It is derived assuming the transmission of equal intensity harmonics through a 150 nm indium filter. (b) Depicts the pulse trains resulting from fourier transforming the spectrum (a) with a relative phase between the harmonics given by equation 5 for different pre-plasma scale-lengths.

harmonics out of the gradient (with  $v_{ph}$  being the local speed of light inside the plasma and  $\Theta_{out,ph}$  the angle under which the harmonics are emitted).

While the photon term can be evaluated using the index of refraction of the plasma  $n(\omega) = \sqrt{1 - \omega_p^2/\omega^2}$ , where  $\omega_p = \sqrt{n_e e^2/\epsilon_0 m_e}$  is the plasma frequency, and only results in a correction factor in the case of a linear density ramp (for the detailed calculation see<sup>24</sup>), the main problem is the treatment of the electron term. Since  $v_e$  and  $\Theta_{in,e}$  are generally unknown parameters and difficult to calculate a reasonable assumption has to be made. While this is not easy for the general case two limits can be treated. For laser intensities of  $a_0 \ll 1$  the electron propagates roughly in the direction of the electric field of the incident laser and its velocity can be estimated using equation  $v_{max} = \frac{eE_0}{\gamma m_e \omega} = \frac{a_0}{\gamma} c$ . In the relativistic limit, i.e. for  $a_0 > 1$ , we can assume  $v_e \approx c$ . For the relativistic case and an angle of incidence of 45 degrees, which is close to the experimental conditions in the measurements reported in<sup>5</sup> equation 4 reduces to

$$\phi(q) = 2\pi \frac{L}{\lambda_L} \frac{n_c}{n_{max}} q^3 (\sqrt{2} + \frac{2}{3}\sqrt{2}). \quad (5)$$

Here the factor of  $\sqrt{2}$  simply originates from the angle of incidence and the  $2/3$  results from the propagation of the harmonics inside the density gradient.

To get a feeling of how this phase relation between the harmonics influences the generated attosecond pulses the results of a model calculation are shown in figure 2. The parameters were chosen to be close to typical experimental conditions under which our measurements of the XUV pulse duration<sup>5</sup> were conducted. For this purpose we assume that all harmonics up to the CWE cutoff are generated with equal intensity on a PMMA target with a peak density of  $n_{\max} = 200 n_c$  and filter this spectrum using the transmission data of a 150 nm indium filter taken from the publication by Henkel et al.<sup>25</sup>. The resulting harmonic power spectrum used in the calculation is shown in figure 2 (a). The spectrum is then fourier transformed to the time domain assuming the phase relation between the harmonics given by equation 5 for different scale-lengths  $L$ . The resulting pulse trains are shown in the various plots of figure 2 (b). The duration of the individual attosecond pulses in the train is also indicated in the figure. Note that for the longest scale-length quoting a full width at half maximum (FWHM) pulse duration does not make much sense because of the multi-peak structure of the pulse train. An interesting evolution of the attosecond pulse duration with the scale length can be observed. With increasing chirp the pulse duration rapidly rises from approximately 400 as to values around 850 as and stays there over a wide range of scale length. For values of  $L$  approaching  $\lambda$  the pulses are distorted so severely that it becomes difficult to identify individual wagons in the train.

Even though this model can, owing to its simplicity and the assumptions made, only give a qualitative picture of the influence of chirp on the attosecond pulses generated via the CWE mechanism it is remarkable how well it seems to reproduce the observed temporal broadening reported in Ref.<sup>5</sup> For reasonable values of the preplasma scale length  $0.05\lambda$  and  $0.25\lambda$  the pulse duration deduced from the model is, to within the experimental accuracy, close to the measured value of roughly 900 as.<sup>5</sup> It is also interesting to note that corrections in the electron velocity and AOI will only change the magnitude of the chirp slightly. It does not have any influence on the functional behavior of the phase with  $q$ . One possibility to increase the precision of the model could be to extract the electron velocity and AOI from a PIC simulation and enter those values into equation 4.

To further support the results obtained with the model calculations we have performed a series of PIC-simulations to study the properties of the emitted harmonic radiation. To visualize the chirp of the harmonic emission, we have post-processed the simulation results by performing a wavelet analysis.<sup>26</sup> The frequency-time diagram for a low intensity driving pulse ( $a_L = 0.2$ ) along with the reflected field and the resulting attosecond pulse train is shown in figure 3 (a) and (b). It is clearly seen in this case that the CWE harmonics exhibit a substantial chirp manifested by the inclination of the harmonics with respect to the time axis with higher harmonics being emitted later as predicted by the model. The chirp also results in significant broadening of the individual as-pulses.

As this broadening is not desirable when the shortest as-pulses are required for an application it is interesting to also investigate the chirp of harmonics generated via the ROM mechanism at relativistic intensities, i.e. when  $a_L \gg 1$ . In this case the underlying physics leading to the generation of the harmonics is the relativistic Doppler frequency shift of an EM-wave back-reflected by a surface moving at velocities close to the speed of light. The interaction of intense laser pulses with plasma results in forced oscillations of the electrons bound to the slowly moving ions. When the laser pulse is reflected by these electrons, it undergoes a frequency up-shift and a spectrum is generated encompassing frequencies up to the roll-over frequency  $\omega_{ro}^{ROM} \propto \gamma_{\max}^3$  where  $\gamma_{\max} \approx a_L$  for  $a_L \gg 1$  is the relativistic Lorentz factor.<sup>2</sup> In this simplified picture of the ROM mechanism, intuitively one expects the harmonics to carry an atto chirp because the reflection occurs at different times and speeds, which results in a time-varying Doppler upshift. However, as it has been pointed out by Baeva et al.,<sup>2</sup> the emission occurs in the neighborhood of the so-called relativistic  $\gamma$ -spikes, the width of which varies as  $1/\gamma_{\max}$ . At high intensities, i.e. high values of  $\gamma_{\max}$ , these  $\gamma$ -spikes tend to be very narrow in time and symmetric so that no appreciable chirp contribution arises. This picture is supported by a detailed analytical treatment, which shows that the phases of the harmonic emission are proportional to the harmonic order.<sup>2</sup> Therefore, in case of ROM harmonics, the harmonic chirp should be negligible.

This prediction is verified by the simulations shown in figure 3 (c) and (d) for high intensities ( $a_L = 10$ ) where the harmonic generation is dominated by the ROM mechanism. In contrast to the low-intensity case no significant chirp is observed (all harmonics are emitted simultaneously) resulting in the generation of significantly shorter as-pulses in this case (compare 3 (b) and (d)). Note that in both cases the harmonic train extracted from the simulation is synthesized from the same harmonic composition containing harmonics 8 to 14.

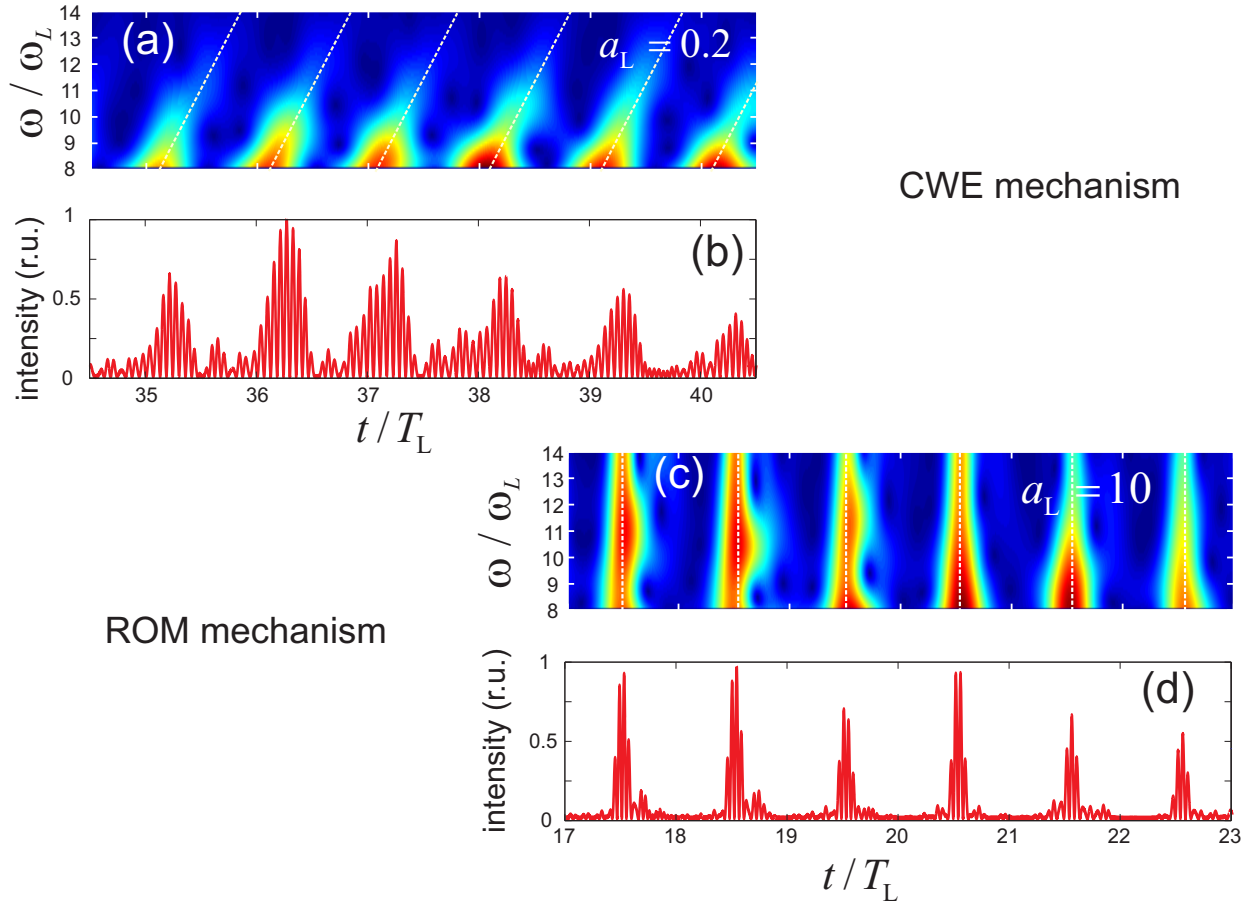


Figure 3. PIC simulations results for a low (panels (a) and (b)) and a high (panels (c) and (d)) intensity case. The simulations were performed with 1D PIC code for the following parameters: laser pulse duration 15 laser cycles, 45 angle of incidence, plasma density 200 overcritical, linear plasma density ramp with scale length and for mobile ions. Panels (a) and (c) show on a linear scale the results of the wavelet analysis of the emission, while panels (b) and (d) the instantaneous intensity of the resulting attosecond pulse train composed of H8 to H14 (red line). The spread of the emission over time of the different harmonics in the range H8 to H14 (inclination denoted by dotted line) in the low intensity case (panel (a)) is a clear indication of atto chirp. In contrast, the high intensity case for the same harmonic range exhibits no discernible atto chirp (panel (c)). As a consequence, the individual attosecond pulse duration differs considerably between the two cases, with the high intensity case delivering shorter pulses.

### 3. CONCLUSIONS

In this paper we have presented a simple model allowing an estimate of the temporal broadening of as-pulses generated from solid surfaces via the CWE mechanism. It is shown that the main source of temporal broadening lies in the fact that different harmonics are emitted from different depth inside the pre-plasma gradient formed during the ionization of the target by the intense laser pulse. Calculations using this model and conducted with parameters close to those of our recent experiment<sup>5</sup> yield as-pulse durations very similar to those obtained experimentally. In addition wavelet analysis of the CWE harmonic emission obtained in 1D PIC simulations at moderate laser intensities ( $a_L = 0.2$ ) supports the predictions of the model and is also in good agreement with the measured results. In contrast to that no chirp is observed in simulations with high intensity pulses ( $a_L = 10$ ) where harmonic generation is dominated by the ROM mechanism supporting theoretical predictions<sup>2</sup> and illustrating the superior phase-locking properties in this regime.

## Acknowledgements

This work was funded in part by the DFG projects Transregio 18 and the MAP excellence cluster and by the Association EURATOM - Max-Planck-Institut für Plasmaphysik. S. G. R. acknowledges financial support from the International Max-Planck Research School on Advanced Photon Science (IMPRS-APS).

## REFERENCES

- [1] Tsakiris, G. D., Eidmann, K., Meyer-ter Vehn, J., and Krausz, F., “Route to intense single attosecond pulses,” *New J. Phys.* **8**, 19 (2006).
- [2] Baeva, T., Gordienko, S., and Pukhov, A., “Theory of high-order harmonic generation in relativistic laser interaction with overdense plasma,” *Phys. Rev. E* **74**(4), 046404 (2006).
- [3] Quéré, F., Thauray, C., Monot, P., Dobosz, S., Martin, P., Geindre, J.-P., and Audebert, P., “Coherent wake emission of high-order harmonics from overdense plasmas,” *Phys. Rev. Lett.* **96**(12), 125004 (2006).
- [4] Krausz, F. and Ivanov, M., “Attosecond physics,” *Rev. Mod. Phys.* **81**, 163–234 (2009).
- [5] Nomura, Y., Hörlein, R., Tzallas, P., Dromey, B., Rykovanov, S., Major, Z., Osterhoff, J., Karsch, S., Veisz, L., Zepf, M., Charalambidis, D., Krausz, F., and Tsakiris, G. D., “Attosecond phase-locking of harmonics emitted from laser-produced plasmas,” *Nat. Phys.* **5**(2), 124–128 (2009).
- [6] Tzallas, P., Charalambidis, D., Papadogiannis, N. A., Witte, K., and Tsakiris, G. D., “Direct observation of attosecond light bunching,” *Nature* **426**, 267–270 (2003).
- [7] Bulanov, S. V., Naumova, N. M., and Pegoraro, F., “Interaction of an ultrashort, relativistically strong laser pulse with an overdense plasma,” *Phys. Plasmas* **1**(3), 745–757 (1994).
- [8] Gordienko, S., Pukhov, A., Shorokhov, O., and Baeva, T., “Relativistic doppler effect: Universal spectra and zeptosecond pulses,” *Phys. Rev. Lett.* **93**(11), 115002 (2004).
- [9] Dromey, B., Zepf, M., Gopal, A., Lancaster, K., Wei, M. S., Krushelnick, K., Tatarakis, M., Vakakis, N., Moustazis, S., Kodama, R., Tampo, M., Stoeckl, C., Clarke, R., Habara, H., Neely, D., Karsch, S., and Norreys, P., “High harmonic generation in the relativistic limit,” *Nat. Phys.* **2**(7), 456–459 (2006).
- [10] Thauray, C., Quéré, F., Geindre, J.-P., Levy, A., Ceccotti, T., Monot, P., Bougeard, M., Reau, F., D’Oliveira, P., Audebert, P., Marjoribanks, R., and Martin, P., “Plasma mirrors for ultrahigh-intensity optics,” *Nat. Phys.* **3**(6), 424–429 (2007).
- [11] Dromey, B., Kar, S., Bellei, C., Carroll, D. C., Clarke, R. J., Green, J. S., Kneip, S., Markey, K., Nagel, S. R., Simpson, P. T., Willingale, L., McKenna, P., Neely, D., Najmudin, Z., Krushelnick, K., Norreys, P. A., and Zepf, M., “Bright multi-keV harmonic generation from relativistically oscillating plasma surfaces,” *Phys. Rev. Lett.* **99**(8), 085001 (2007).
- [12] Tarasevitch, A., Lobov, K., Wuensche, C., and von der Linde, D., “Transition to the relativistic regime in high order harmonic generation,” *Phys. Rev. Lett.* **98**(10), 103902 (2007).
- [13] Dromey, B., Adams, D., Hörlein, R., Nomura, Y., Rykovanov, S. G., Carroll, D. C., Foster, P. S., Kar, S., Markey, K., McKenna, P., Neely, D., Geissler, M., Tsakiris, G. D., and Zepf, M., “Diffraction limited performance and focusing of high harmonics from relativistic plasmas,” *Nat. Phys.* **5**(2), 146–152 (2009).
- [14] Burnett, N. H., Baldis, H. A., Richardson, M. C., and Enright, G. D., “Harmonic generation in CO<sub>2</sub> laser target interaction,” *Appl. Phys. Lett.* **31**(3), 172 (1977).
- [15] Carman, R. L., Rhodes, C. K., and Benjamin, R. F., “Observation of harmonics in the visible and ultraviolet created in CO<sub>2</sub>-laser-produced plasmas,” *Phys. Rev. A* **24**(5), 2649–2663 (1981).
- [16] Bezzerides, B., Jones, R. D., and Forslund, D. W., “Plasma mechanism for ultraviolet harmonic radiation due to intense CO<sub>2</sub> light,” *Phys. Rev. Lett.* **49**(3), 202–205 (1982).
- [17] Teubner, U., Eidmann, K., Wagner, U., Andiel, U., Pisani, F., Tsakiris, G. D., Witte, K., Meyer-ter Vehn, J., Schlegel, T., and Förster, E., “Harmonic emission from the rear side of thin overdense foils irradiated with intense ultrashort laser pulses,” *Phys. Rev. Lett.* **92**(18), 185001 (2004).
- [18] Brunel, F., “Not-so-resonant, resonant absorption,” *Phys. Rev. Lett.* **59**(1), 52 (1987).
- [19] Sheng, Z.-M., Mima, K., Zhang, J., and Sanuki, H., “Emission of electromagnetic pulses from laser wakefields through linear mode conversion,” *Phys. Rev. Lett.* **94**(9), 095003 (2005).

- [20] Quéré, F., Thaury, C., Geindre, J.-P., Bonnaud, G., Monot, P., and Martin, P., “Phase properties of laser high-order harmonics generated on plasma mirrors,” *Phys. Rev. Lett.* **100**(9), 095004 (2008).
- [21] Dromey, B., Rykovanov, S., Adams, D., Hörlein, R., Nomura, Y., Foster, P. S., Kar, S., Markey, K., Neely, D., Geissler, M., Tsakiris, G. D., and Zepf, M., “Tuneable enhancement of high harmonic emission from laser–solid interactions,” submitted.
- [22] Hörlein, R., Nomura, Y., Osterhoff, J., Major, Z., Karsch, S., Krausz, F., and Tsakiris, G. D., “High harmonics from solid surfaces as a source of ultra-bright xuv radiation for experiments,” *Plasma Phys. Control. Fusion* **50**, 124002 (2008).
- [23] Thaury, C., George, H., Quéré, F., Loch, R., Geindre, J.-P., Monot, P., and Martin, P., “Coherent dynamics of plasma mirrors,” *Nat. Phys.* **4**(8), 631–634 (2008).
- [24] Nomura, Y., *Temporal characterization of harmonic radiation generated by intense laser-plasma interaction*, PhD thesis, Ludwig-Maximilians-Universität München (2008).
- [25] Henke, B. L., Gullikson, E. M., and Davis, J. C., “X-ray interactions: photoabsorption, scattering, transmission, and reflection at  $e=50$ -30000 eV,  $z=1$ -92,” *Atomic Data and Nuclear Data Tables* **54**(2), 181–342 (1993).
- [26] Rykovanov, S. G., Geissler, M., Meyer-ter Vehn, J., and Tsakiris, G. D., “Intense single attosecond pulses from surface harmonics using the polarization gating technique,” *New J. Phys.* **10**, 025025 (2008).